JOURNAL OF OPTOELECTRONICS AND ADVANCED MATERIALS Vol. 8, No. 5, October 2006, p. 1770 - 1774

Inductive response of ferrites based on resonance effects

N. KONTOS, A. KTENA[a], T. SOFIANOPOULOU, E. HRISTOFOROU[*]
School of Mining and Metallurgy Engineering, National Technical University of Athens, Zografou Campus, Athens 15780, Greece
[a]*Department of Electrical Engineering, TEI of Chalkis, Psahna Euboea, 34400, Greece*

A method and a setup are presented that allow the investigation of the magneto-inductive phenomenon in the development of position, stress and field sensors, as well as in studying fundamental properties of the used ferromagnetic materials. The phenomenon of resonance in a series RLC circuit is used to study the effect of displacement of the soft ferrite core of the inductor on the peak output voltage across the resistor at resonance. More specifically, the displacement of the core affects the inductance of the circuit and therefore the resonance frequency and the peak output voltage. Several ferrite samples have been used having undergone treatments such as oxidization, annealing and corrosion. The same RLC circuit has also been used to study the effect of applied tensile stress and magnetic field at various frequencies when the core of the inductor is a 25cm long ribbon made of an iron alloy. In this case, the resonance frequency is constant and the output voltage across the resistor is recorded as a function of frequency, stress, and magnetic field. In both cases, the results are correlated to the permeability of the core and the way its permeability changes with respect to the applied stress or field, the frequency of excitation, the treatment it has undergone and its magnetic history. Thus, the presented system may also serve as a tool for determination of the electric and magnetic properties of the under test samples.

(Received September 9, 2006; accepted September 13, 2006)

Keywords: Inductive response, Resonance, Permeability

1. Introduction

Magnetic sensors play a significant role in physical measurements used in all kinds of applications [1, 2]. The most often used magnetic phenomena in today's magnetic sensor technology are the magneto-resistance [3,4], the magneto-impedance [5, 6], the magnetostriction [7, 8], the electromagnetic induction [9] and the Hall effect [10]. There also exist other effects usable in sensing applications, both macroscopic and microscopic [11].

A series RLC circuit and the phenomenon of resonance have been the basis on which the sensing principle presented in this paper is based [12]. A series RLC circuit consists of a resistor R, a capacitor C and an inductor L with a metallic magnetic core (Fig. 1). In the case of a sinusoidal excitation $V(t) = V_{\max} \sin \omega t$, the Kirchhoff's second law for that circuit is $Ri + L\frac{di}{dt} + \frac{1}{C}\int idt = V(t)$. The steady-state solution of this integro-differential equation yields a current given by $i(t) = \frac{V_{\max}}{Z}\sin\left(\omega t + \tan^{-1}\frac{X}{R}\right)$ where Z is the equivalent complex resistance of the circuit $Z = \sqrt{R^2 + X^2}$ and X is the equivalent imaginary reactance $X = \omega L - \frac{1}{\omega C}$. The voltage across the resistor R is then equal to $V_R(t) = R \cdot i(t)$. $V_R(t)$ is a function of the circuit impedance Z which is a function of the circuit components R, C, and L and the excitation peak voltage V_{max} as well as of the excitation frequency $\omega = 2\pi f$. The field and stress sensors presented in this paper utilize this dependence.

In resonance, the current i(t) is maximized because Z is minimized. This is due to the fact that the circuit reactance decreases to zero: $\omega L = \frac{1}{\omega C} \Leftrightarrow \omega = \frac{1}{\sqrt{LC}} = \omega_0$ where ω_0 is the resonance frequency. The resonance frequency depends solely on the components L, C.

The value of the inductance depends on the construction of L as well as on the presence of a core. Iron cores are used in inductors to increase the magnetic flux density inside it. Soft ferrites are typically used as core materials in inductors in band-pass filters because of their high resistance and electrical permeability combined with high magnetic permeability, high saturation magnetization and low coercivity. Their electrical properties guarantee low eddy current losses in high frequency applications while their magnetic properties allow for high flux density and the development of strong magnetic fields inside the inductors. Ferrites are ceramic alloys of the type MO Fe_2O_3 where MO are oxides of some transition metal such as Mn, Ni or Mg.

2. Experiment

2.1. Position and displacement measurements

A series RLC circuit, as the one shown on Fig. 1, is constructed with the following components: a standardized resistor R = 12.2 Ω, a capacitor C = 1 μF and an inductor of length 19.5 cm, mean diameter 1.14 cm and 975 turns with a core-less inductance of $L_0 = \mu_0 N^2 \cdot \frac{S}{\ell} = 0.6244$ mH. The resonance frequency in the absence of a core is f = 40.02 kHz. A frequency generator supplies the excitation voltage V(t) while the voltage V_R is recorded by a digital oscilloscope. Inserting a ferrite core inside the inductor increases its inductance because it increases the magnetic permeability μ of the inductor. When the core is at a distance *x* from the end of the inductor as shown in Fig.1 the total inductance is the sum of two inductances L(x) = L_1 + L_2 where $L_1 = \frac{\ell - x}{\ell} \cdot L_0$ and $L_2 = \mu \frac{x}{\ell} \cdot L_0$, where μ is the magnetic permeability of the ferrite core.

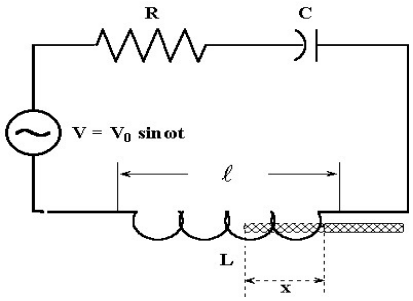

Fig. 1. Series RLC circuit for the position and displacement sensor.

The output voltage across the resistor V_R depends therefore on the position of the core as well as on the magnetic permeability of the core. Several nickel ferrite samples (spinels) of the type $NiO \cdot Fe_2O_3$ have been used with a composition of Fe_xO_y: 66.71%, NiO: 12.76% and ZnO: 20.53%. The zinc oxide helps to further increase the electrical resistance of the alloy, thus suppressing the eddy currents and reducing the related losses in high frequencies (> 10MHz). Twelve samples have been prepared and tested in total. Some of them underwent treatments of oxidation, annealing and corrosion. Their resulting structures were observed in the electronic microscope. The oxidation process took place in 350ºC for one hour in an oxidation furnace. Corrosion was realized by submerging the samples in 96% H_2SO_4 for 10 min., 20 min., 30 min. and 1h. In order to relieve the samples of any internal stresses built in during the preparation and post-processing, they were annealed in 500 ºC in an Ar atmosphere for two hours followed by a 5-hour cooling period down to 200 ºC.

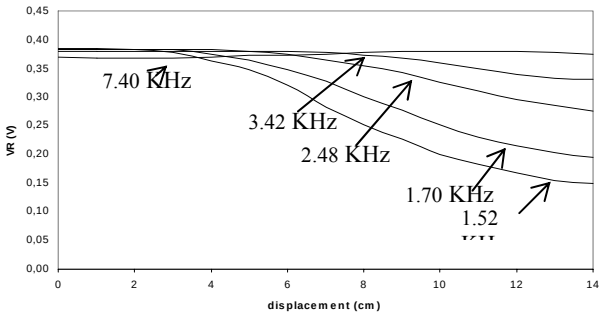

Fig. 2. As cast ferrite sample.

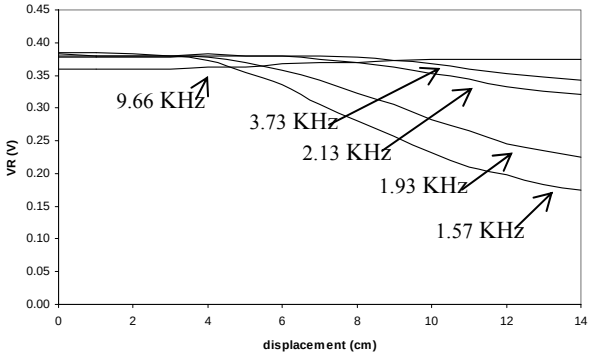

Fig. 3. Oxidized and annealed sample.

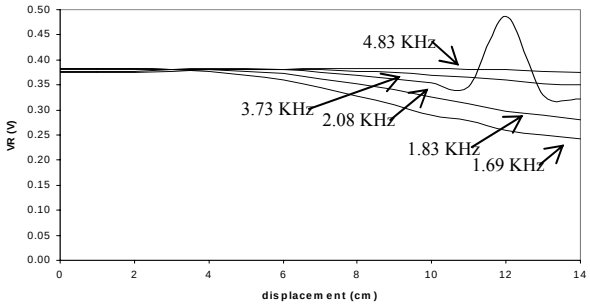

Fig. 4. Sample exposed to corrosion for 1h.

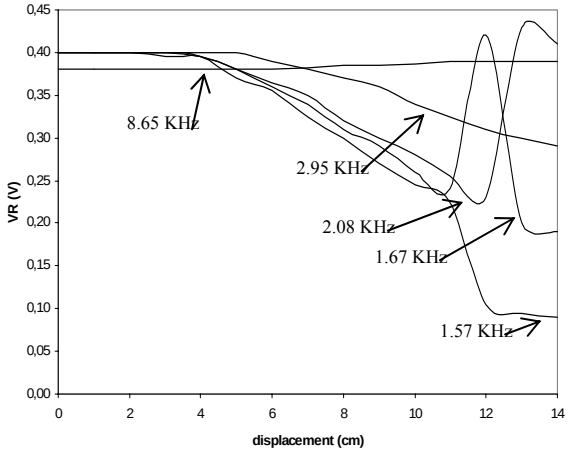

Fig. 5. Annealed sample exposed to corrosion for 10 min.

The following experimental procedure was realized: each sample was inserted fully into the inductor; the circuit was brought to resonance by altering the excitation frequency and the peak voltage V_R at resonance and the resonant frequency were recorded. Then the sample was taken out of the inductor in steps of 1 cm recording the peak voltage each time. A total of 14 steps were involved. The above procedure was repeated for 13 more frequencies corresponding to the resonant frequencies at each step. The responses of several samples are shown on Figs. 2-5.

2.2. Stress and field measurements

The series RLC circuit used for the stress and field sensor consisted of an 1 Ω resistor, a 10 μF capacitor and a 2 mH inductor. The circuit operated under a sinusoidal voltage V(t) = 20 sin ωt and the voltage V_R across the resistor was monitored on the scope. For a core-free inductor, the resonance is at f_0 = 1125 Hz. A metallic ribbon made of a FeMnCuNi alloy is used as core. The core is 25 cm long and is subjected to tensile stress.

For each set of measurements, the frequency was kept constant while the applied stress was varied from 5-150 MPa. The peak output voltage is recorded for the above-mentioned range of stresses at several operating frequencies. The results are shown in Figs. 6-8.

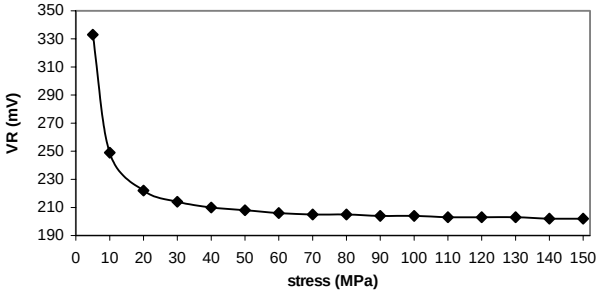

Fig. 6. The peak output voltage dependence on applied stress at 10 Hz.

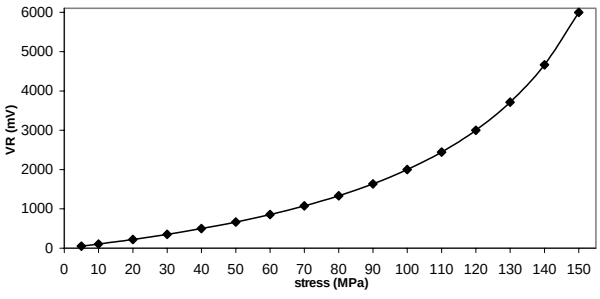

Fig. 7. The peak output voltage dependence on applied stress at 1 kHz.

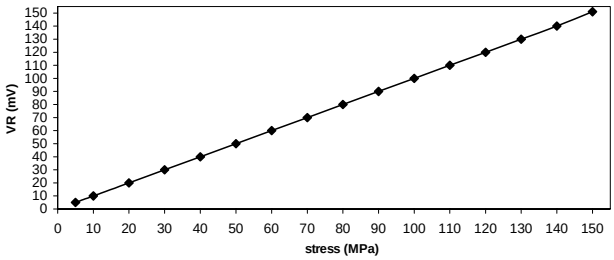

Fig. 8. The peak output voltage dependence on applied stress at 10 kHz.

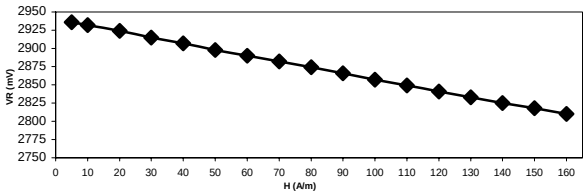

Fig. 9. The peak output voltage dependence on applied magnetic field at 10 Hz.

Finally, the same setup with the same core under zero stress was used to examine the V_R response with respect to an applied magnetic field at several frequencies. Similarly to the previous experiment, for each set measurements, the frequency was kept constant while the field was varied from 5-160 A/m as shown in Figs. 9-10.

3. Discussion

The results for the position sensor are shown in Figs. 2-5, showing the peak output voltage dependence on the core displacement in the case of an as cast sample, an oxidized and subsequently annealed sample, one sample that underwent corrosion for 1h and one that was exposed to corrosion for 10'and then annealed. In all cases, there is a plateau region for the first 3-4 cm of the core displacement followed by a monotonic and linear decrease of the output voltage as the core is progressively taken out of the inductor. As the core leaves the inductor, its inductance L decreases and so does the corresponding inductive reactance X_L which no longer cancels out with the capacitive reactance X_C. The circuit's equivalent impedance $Z = \sqrt{R^2 + (X_L - X_C)^2}$ is capacitive (since $X_C > X_L$) and higher than R. As a result, as the circuit's behavior gets increasingly further away from the state of resonance, the circuit's current decreases and so is V_R. When the core displacement is at 14 cm, the output voltage reaches the minimum value, corresponding to the reponse of a coreless inductor. As the frequency decreases, the decrease in the voltage becomes increasingly smaller which suggests that the sensitivity of such a sensor is maximized when operated at the frequency f_0, the

resonance frequency when no displacement is taking place. This is because, the circuit's inductive (capacitive) reactance increases rapidly at frequencies higher (lower) than the resonant frequency; hence, the current decreases and so does the output voltage V_R. In some cases of oxidized and corroded samples, a non-monotonic behavior is observed (Fig. 5) for a given frequency. This sudden increase in V_R suggests that resonance occurs at that given frequency and position corresponding to a minimization of the magnetic permeability of the sample for that given frequency. The samples that have undergone some treatment such as annealing or corrosion yield higher voltage values, suggesting the important role the microstructure plays in the sensor's behavior. Among others, the post processing of the samples affects their magnetic permeability and the subsequent resonant frequencies (Fig 11). It can be found that the magnetic permeability μ is a function of the operating frequency ω and is given by the equation:

$$\mu(\omega) = \frac{l}{x}\left(\frac{V_0 - V_R}{V_R}\frac{R}{\omega L_0} + \frac{1}{\omega^2 L_0 C} - 1\right) + 1$$

where V_0 is the peak value of the excitation voltage, L_0 the inductance of the core free inductor, V_R the voltage across the resistor R, C the capacitor, l is the length of the inductor and x the displacement of the core. The above relationship can also yield the ac susceptibility χ_{ac} of the core since it is known that $\chi_{ac}(\omega) = 1 - \mu(\omega)$. Thus, the frequency dependence of both the susceptibility χ and the permeability μ of the core can be experimentally determined.

In the case that $\omega = \omega_0 = \frac{1}{\sqrt{L_0 C}}$, *i.e.* the resonance frequency for a core free inductor,

$$\mu(\omega_0) = \frac{l}{x}\frac{V_0 - V_R}{V_R}\frac{R}{\omega_0 L_0} + 1.$$

In the limiting case that $x=l$, *i.e.* the core is fully inserted in the inductor,

$$\mu(\omega) = \frac{V_0 - V_R}{V_R}\frac{R}{\omega L_0} + \frac{1}{\omega^2 L_0 C}$$

From the above analysis, it can be seen that the magnetic permeability μ is inversely proportional to the voltage across the resistor R, the operating frequency ω and the core displacement x.

As the length of the core inside the inductor decreases, its measurable magnetic permeability decreases since the demagnetizing fields of the core increase. Software techniques may be used to determine the demagnetization factor or compensate for the demagnetizing field.

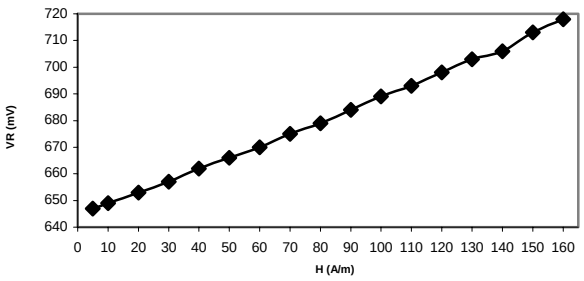

Fig. 10. The peak output voltage dependence on applied magnetic field at 100 Hz.

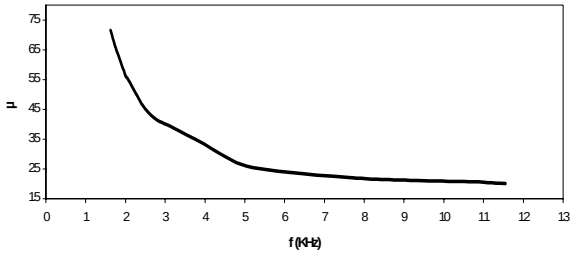

Fig. 11. The magnetic permeability dependence on frequency.

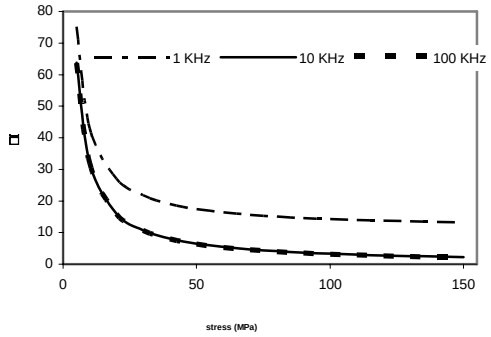

Fig. 12. The magnetic permeability dependence on applied tensile stress.

Concerning the position response of the proposed arrangement, the sharp and non-monotonic response of some samples at some frequencies can be used for dilatometric sensing elements due to their highly sensitive response.

The annealing study showed that the lower the frequency, the lower the sensitivity as well as the aging effect. Therefore, high frequency operation is suggested when higher sensitivity is required. However, in that case attention should be paid to the aging behavior of the material, *e.g.* the use of plastic coatings should be considered.

Figs. 6-8 show the response of the stress sensor as the output voltage dependence on applied tensile load at various frequencies. For frequencies higher than several thousand Hz, the sensor response is linear (Fig. 8). Around 10 Hz, it is a negative exponential (Fig. 6) while at higher frequencies and up to a few kHz it is a positive exponential (Fig. 7). In the high frequency regions, the circuit impedance Z is very high and therefore the current

and ensuing voltage V_R across the resistor R are low. This explains why the response in these frequencies yields low voltage values, of several tens of mV, and appears to be linear. As we approach resonance, the output voltage is maximized, reaching several V, the positive exponential behavior of the response increases and so does the sensitivity (Fig. 7). Below resonance, the circuit's impedance turns capacitive and therefore the sign of the exponential changes to negative. The higher sensitivity of the response is attributed to the higher sensitivity of permeability on the applied stress at low frequencies (Fig. 6).

Fig. 12 shows the magnetic permeability dependence on the applied load for several frequencies. The permeability μ is decreasing exponentially with the applied load tending to a constant value beyond 60 MPa. Therefore, this arrangement could be used for the development of a very sensitive stress sensor appropriate for low load applications.

A similar behavior is observed in the case of the field sensor arrangement (Figs. 9- 10), illustrating that stress behaves like an effective field for a wide frequency range.

4. Conclusions

The inductive response of appropriate inductor cores in a series RLC circuit has been investigated with respect to its potential as a sensing principle. It has been shown that the displacement of a ferrite core inside the inductor of the circuit can result in a sensitive position and displacement sensor and even a dilatometer if operated at the appropriate frequency. The same arrangement yields a rather straight forward method of measuring the ac susceptibility and the permeability of the material as well. Keeping the core in place while applying stress or magnetic fields to it, results in a stress and field sensor, respectively.

References

[1] G. Brumfiel, Nature **426**(6963), 110 (2003).
[2] E. Hristoforou, J. Optoelectron. Adv. Mater. **4**(2), 245 (2002).
[3] Bakonyi, L. Peter, V. Weihnacht, J. Toth, L. F. Kiss, C. M. Schneider, J. Optoelectron. Adv. Mater. **7**(2), 589 (2005).
[4] V. Georgescu, M. Daub, J. Optoelectron. Adv. Mater. **7**(2), 853 (2005).
[5] J. M. Barandiaran, M. L. Fdez-Gubieda, J. Gutierrez, I. Orue, A.G. Arribas, G.V. Kurlyandskaya, J. Optoelectron. Adv. Mater. **6**(2), 565 (2004).
[6] L. V. Panina, D. P. Makhnovskiy, K. Mohri, J. Magn. Magn. Mater. **272,** 1452 (2004).
[7] H. C. Jiang, W. L. Zhang, W. X. Zhang, S. Q. Yang, H. W. Zhang, J Mater. Sci. Technol. **21**(3), 315 (2005).
[8] P. Ciureanu, G. Rudkowska, L. Clime, A. Sklyuyev, A. Yelon, J. Optoelectron. Adv. Mater. **6**(3), 905 (2004).
[9] D. de Cos, A. Garcia-Arribas, J.M. Barandiaran, Sensor Actuat. A – Phys. **112**(2-3), 302 (2004).
[10] G. Boero, I. Utke, T. Bret, N. Quack, M. Todorova, S. Mouaziz, P. Kejik, J. Brugger, R.S. Popovic, P. Hoffmann, Appl. Phys. Lett. **86**(4), 042503 (2005).
[11] H. Chiriac, M. Tibu, V. Dobrea, I. Murgulescu, J. Optoelectron. Adv. Mater. **6**(2), 647 (2004).
[12] N. Kontos, Final Year Dissertation, National Technical University of Athens, 2001.

*Corresponding author: eh@metal.ntua.gr